Armenian Journal of Physics, 2011, vol. 4, issue 1, pp. 30-37

FALICOV-KIMBALL MODEL EXTENDED BY ELECTRON-PHONON INTERACTION (EPI)

S. K. Bhowmick, N. K. Ghosh*

Department of Physics, University of Kalyani, Kalyani-741235, WEST BENGAL, INDIA

E-mail: nanda.ku@rediffmail.com

Received 15 June, 2011

Abstract–The effect of electron-phonon interaction (EPI) has been investigated using extended Falicov-Kimball model in an exact method. Phonon-induced hybridization term is considered in terms of electron operators. Average occupation number off-electrons, entropy, specific heat, and spin susceptibility are calculated. First-order valence transition occurs at an increased value of EPI. Double-peak structure is observed in specific heat curves. The specific heat coefficient g rises sharply at low temperatures. EPI increases the rate of growth of antiferromagnetic correlations.

Keywords: Mixed valent systems; Falicov-Kimball model; electron-phonon interaction

1. Introduction

The Falicov-Kimball model (FKM) [1] was initially introduced as a statistical model to describe metal-insulator transition in rare-earth and transition metal compounds. Later, it is extensively used to capture the ingredients of alloy formation, mixed valence, and ferroelectricity [2–5]. Both spinless and spin-versions of the FKM have been used to describe pressure or temperature induced valence transitions in rare-earth mixed-valence (MV) compounds which are characterised by the presence of the rare-earth ion in two valence states, the $4f^n$ and $4f^{n-1}$ ionic configurations. Anomalies in the physical properties of these rare-earth compounds result from a change in the occupation numbers of the electronic states. The list of rare-earth compounds (compounds with Sm, Tm, Ce, Eu) and transition metal compounds (compounds with Fe, Ti, V) is long. Resistivity and optical experiments on Sm compounds (SmS, SmSe and SmTe) demonstrate a pressure induced semiconductor to metal transition due to a change of valence of the samarium ions [6]. Mossbauer isomer shift measurements show that Sm valence changes from 2 at normal pressure to an intermediate value of about 2.8 in the metallic phase [6].

A number of realistic extensions of the FKM have been examined to explain the anomalous features. Finite temperature valence transition is investigated [7] using extended FKM with Coulomb repulsion and the electron-phonon interaction (EPI). The ground state properties of the model have been changed appreciably when the correlated hopping term is included [8]. Correlated hopping interaction induced discontinuous insulator to metal transition is observed at a critical f-level energy [9]. The influence of nonlocal Coulomb interaction within the model has been studied using small-cluster exact diagonalization method and it is shown that the interaction substantially changed the f-electron distributions, the valence transitions, as well as the conducting properties of the model [10].

When the electronic configuration changes from $4f^n \rightleftharpoons 4f^{n-1}$, the radii of rare-earth ions vary significantly and therefore excitation of lattice degrees of freedom occurs, and so the EPI is expected to play an important role in MV phenomena [11]. There are strong evidences in favour of the presence of EPI from experimental observations. Polaronic features are observed in optical conductivity [12] and the angle-resolved photoemission experiments (ARPES) [13]. Evidence of strong EP coupling are provided by tunneling experiments [14]. Observed 'kink' in the electronic dispersions of the ARPES experiments can be explained by the presence of phonons [15].

A large number of theoretical studies have been done on the role of EPI in MV phenomena [16-18]. In most of the works, the effect of EP coupling has been seen as a renormalization of the bare electronic interactions. In [16], applying mean field approximation, authors showed that phonon-induced f-f and f-d couplings make the first-order transition as observed in SmS. The effects of phonon-induced hybridization on valence transition, specific heat and magnetic intersite spin correlations are studied in [17]. Reducing the EPI to the phonon-mediated f-f interaction by a canonical transformation, authors showed that spin-1/2 FKM could describe correctly the physics of intermediate-valence systems [18]. Many physical properties of high-T_c cuprates can be explained using EPI, in particular the high critical temperature T_c, the anomalous isotope effect, the superconducting gap etc. [19].

Results on the studies of valence and insulator-metal transitions are largely dependent on the approximations used [16, 20, 21]. Various approximations yield diverse and contradictory results. Here lies the importance of the studies using exact methods. In the present work, to describe the effect of EPI in MV phenomena, EPI induced hybridization term has been taken in the FKM. Considering a 2D four-site square cluster and using finite cluster exact diagonalization calculations, we have examined the effects of EPI on entropy, specific heat and spin susceptibility. A comparison has also been made with existing results.

2. Formulation

Menezes and Troper [11] considered the following model Hamiltonian

$$H = H^{el} + H^{ph} + H^{el-ph}, \tag{1}$$

where H^{el} is the pure electronic part, H^{ph} is the pure phononic contribution and H^{el-ph} is the generalized EPI. Using displacement operator technique, the Hamiltonian (1) has been transformed in terms of electron operators. Neglecting wave vector dependence and considering only $\mathrm{d} \rightleftharpoons \mathrm{d}$ and $\mathrm{f} \rightleftharpoons \mathrm{d}$ couplings in the EPI (neglecting $\mathrm{f} \rightleftharpoons \mathrm{f}$ one as f-electrons are highly localized), we have used the EPI induced hybridization term of this transformed Hamiltonian in the form

$$H_v = V \sum_{\langle i,j \rangle \sigma} \left(f_{i\sigma}^{\dagger} d_{i\sigma} + d_{i\sigma}^{\dagger} f_{i\sigma} \right) - g \sum_{\langle i,j \rangle \sigma\sigma'} n_{i\sigma'}^{d} \left(f_{i\sigma}^{\dagger} d_{i\sigma} + d_{i\sigma}^{\dagger} f_{i\sigma} \right). \tag{2}$$

The EP coupling constant $g = 2\pi g_{fd} g_{dd} / h\omega$, where g_{fd} and g_{dd} are the $f \rightleftharpoons d$ and $d \rightleftharpoons d$ EP coupling constants respectively, *h* is the Planck's constant, and V is the f-d hybridization parameter.

Now the Hamiltonian we have considered in this problem is

$$H = H_0 + H_v + H_{corr}, \tag{3}$$

where

$$H_0 = E\sum_{i\sigma} f_{i\sigma}^{\dagger} f_{i\sigma} + U\sum_{i} f_{i\uparrow}^{\dagger} f_{i\uparrow} f_{i\downarrow}^{\dagger} f_{i\downarrow} + G\sum_{i\sigma\sigma'} d_{i\sigma}^{\dagger} d_{i\sigma} d_{i\sigma'}^{\dagger} d_{i\sigma'} + t\sum_{\langle i,j\rangle\sigma} d_{i\sigma}^{\dagger} d_{i\sigma}, \tag{4}$$

where $\langle i, j\rangle$ are all pairs of nearest-neighbors site on the two-dimensional square lattice; $f_{i\sigma}$ and $d_{i\sigma}$ are the usual fermions' operators for f- and d- electrons respectively $(\sigma, \sigma' = \text{spin})$, E is the f-level energy, *G* is the strength of the f-d Coulomb interaction, *U* is the on-site Coulomb interaction. The last term corresponds to quantum-mechanical hopping of the itinerant d-electrons between nearest-neighbor sites.

$$H_{corr} = t'\sum_{\langle i,j\rangle\sigma} \left(f_{i\sigma}^{\dagger} f_{i\sigma} + f_{j\sigma}^{\dagger} f_{j\sigma} \right) d_{i\sigma}^{\dagger} d_{j\sigma}, \tag{5}$$

where H_{corr} is the correlated hopping term with interaction strength t'.. The representative four-site spin state is taken in the form [9]

$$\left| n_{1\uparrow}^{f} n_{1\downarrow}^{f} n_{1\uparrow}^{d} n_{1\downarrow}^{d} n_{2\uparrow}^{f} n_{2\downarrow}^{f} n_{2\uparrow}^{d} n_{2\downarrow}^{d} n_{3\uparrow}^{f} n_{3\downarrow}^{f} n_{3\uparrow}^{d} n_{3\downarrow}^{d} n_{4\uparrow}^{f} n_{4\downarrow}^{f} n_{4\uparrow}^{d} n_{4\downarrow}^{d} \right\rangle \tag{6}$$

There are altogether 120 basis states. In our exact diagonalization study, the ground state is taken in the form

$$\left|\psi\right\rangle = \sum_{m} c_m \left|\psi_m\right\rangle. \tag{7}$$

The coefficients c_m are the solutions of the system of equations

$$M \begin{pmatrix} c_1 \\ \vdots \\ c_N \end{pmatrix} = 0, \tag{8}$$

where *N* is the dimension of the Hilbert space and *M* is a symmetric matrix with a typical element as

$$M_{mn} = \left[\left\langle \psi_m \middle| H \middle| \psi_n \right\rangle - \lambda\delta_{mn} \right]. \tag{9}$$

λ being the lowest solution of the eigenequation

$$\det M = 0 \tag{10}$$

and $\left|\psi_m\right\rangle$, $\left|\psi_m\right\rangle$ are the basis states. The f-electron density $\left\langle n_i^f \right\rangle = (1/N)\sum_{i\sigma} f_{i\sigma}^{\dagger} f_{i\sigma}$. Entropy per lattice site is given by

$$S = (1/N)\left(k_B \ln Z + \langle H\rangle / T\right). \tag{11}$$

Low temperature specific heat is calculated using the relation

$$C = k_B \beta^2 \frac{\partial^2}{\partial \beta^2} \ln Z, \tag{12}$$

where $Z = \sum_\alpha e^{-\beta E_\alpha}$, the sum is taken over all eigenstates, E_α's are the corresponding eigenvalues, and $\beta = 1/k_B T$, k_B is the Boltzmann constant (taken as unity throughout our calculations). Spin susceptibility for f-electrons is taken as

$$\chi = \beta \left\langle \left(n_{i\uparrow}^f - n_{i\downarrow}^f \right)^2 \right\rangle. \tag{13}$$

3. Results and Discussions

The effect of EPI on valence transition is shown in Figure 1. The first-order transition occurs at an increased value of *g*. The effective hybridization $\tilde{V}$ ($\tilde{V} = V - g\left\langle n^d \right\rangle$) decreases with the increase of g causing an abrupt transition at some lower critical value of $\tilde{V}$. The jump of $\left\langle n_i^f \right\rangle$ is from a value close to 0.5 to a value close to zero, because weaker hybridization keeps $\left\langle n^d \right\rangle$ smaller before the transition. This result is in agreement with renormalization group results [22], the alloy analog approximation [23] and small-cluster exact-diagonalization calculations [24]. Thus EPI enhances the tendency to an abrupt transition [16].

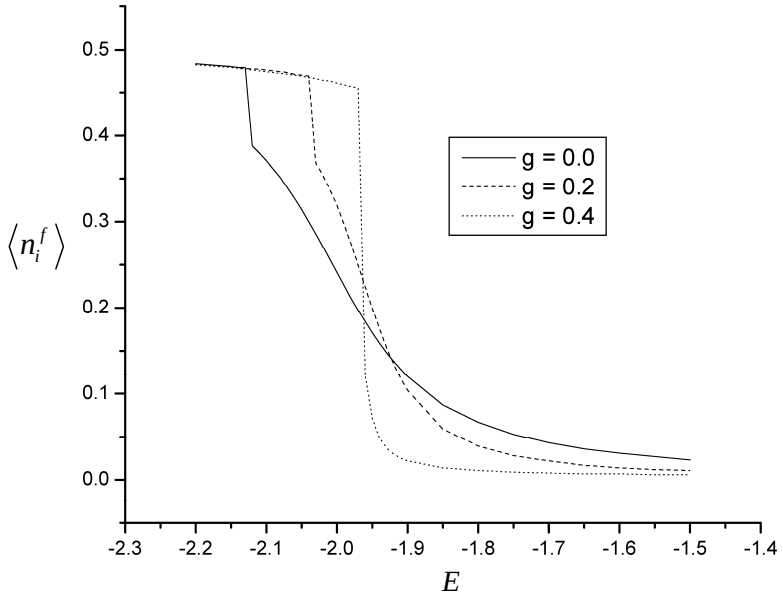

Fig. 1. Variation of $\left\langle n_i^f \right\rangle$ with *E* for different *g*. Here *V* = 0.1, *U* = 2.0, *G* = 1.0, *t*' =0.1, *t* = –1.0.

Figure 2 shows the dependence of entropy on temperature for different g. It is apparent that with the increase of EPI upto a range of physical interest, we get more ordered state. Thus, the inclusion of EPI has important effects in MV phenomena. As the temperature increases, the

difference between different g curves becomes broad. The transition temperature region is identified as $0.05 < T < 0.5$ (approximately), where the difference between the curves is maximum [25]. The curves show good convergence for $T > 0.5$.

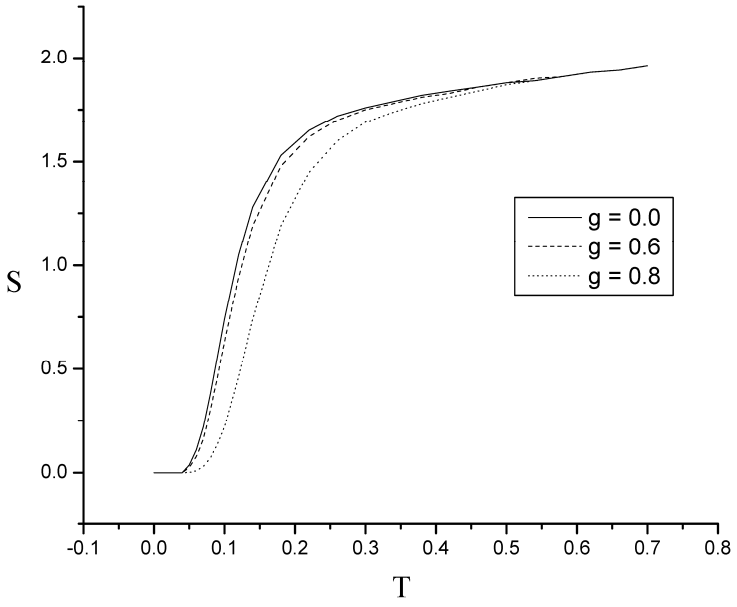

Fig. 2. Entropy vs. temperature for different *g*. Here $E = -1.8$, $V = 0.1$, $U = 2.0$, $G = 1.0$, $t' = 0.1$, $t = -1.0$.

The specific heat curves in Figure 3 exhibit a double peak structure [26]-one sharp peak followed by a broad peak. A large number of many body states, degenerate with the ground state, are responsible for the origination of the first sharp peak. The broad peak at higher temperature is of Schottky type. With the increase of EPI, the peak value of specific heat increases and appears at higher temperature. It is apparent from the figure that EPI decreases effective hybridization which in turn increases density of states at the lower temperatures.

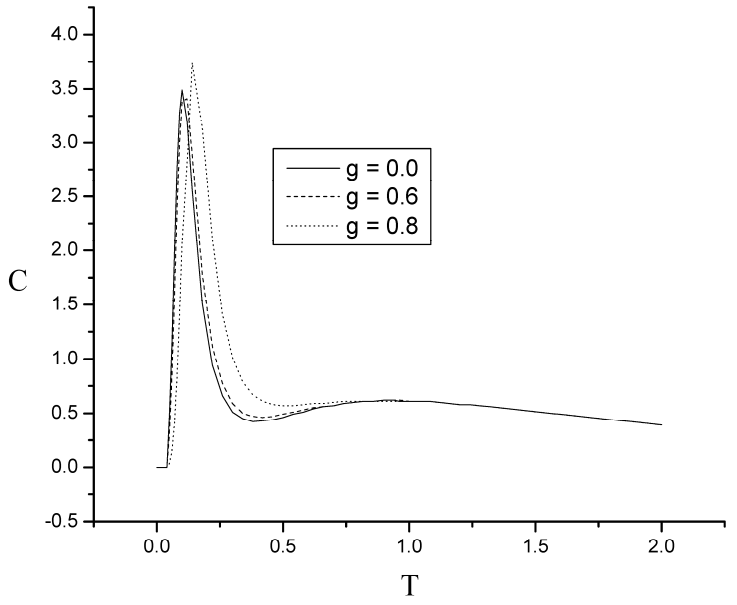

Fig. 3. Specific heat vs. temperature for different *g*. Here $E = -1.8$, $V = 0.1$, $U = 2.0$, $G = 1.0$, $t' = 0.1$, $t = -1.0$.

In Figure 4, we have shown the variation of specific heat coefficient γ against *T*. γ exhibits a single peak structure and is enhanced sharply at low temperatures. This sharp rise of γ is due to the presence of more many body states, degenerate with the ground state. Peak value of γ decreases with EPI. Comparing Figure 4 with Figure 3, it appears that *g* increases phononic contribution to specific heat ($C = \gamma T + \beta T^3$ where γ and β are the coefficients for the electronic and phononic contributions to specific heat, respectively [27]). So, EPI prevents the onset of heavy-fermion behavior [28].

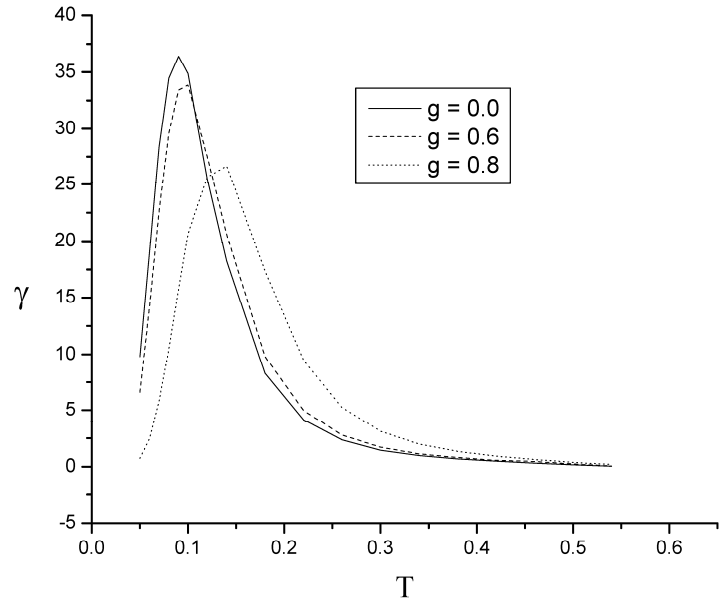

Fig. 4. Specific heat coefficient vs. temperature for different *g*. Here $E = -1.8$, $V = 0.1$, $U = 2.0$, $G = 1.0$, $t' = 0.1$, $t = -1.0$.

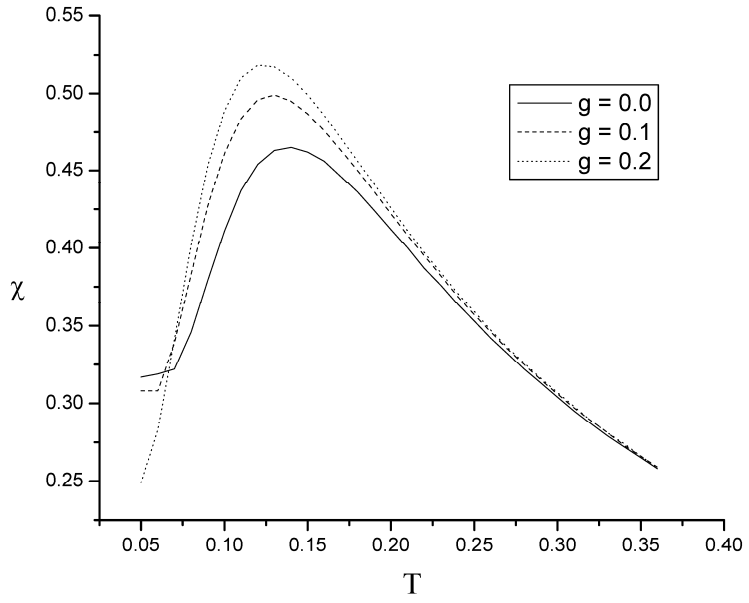

Fig. 5. Variation of spin susceptibility with temperature for different *g*. Here $E = -1.8$, $V = 0.1$, $U = 2.0$, $G = 1.0$, $t' = 0.1$, $t = -1.0$.

In Figure 5 we show the spin susceptibility χ as a function of T. At the lower temperatures, the spin susceptibility is small due to the presence of spin gap [29]. Susceptibility increases with temperature, attains a peak value, and then decreases. With the increase of EPI, the peak value of susceptibility increases. The peak in χ signals the onset of short range antiferromagnetic order. EPI increases the rate of growth of antiferromagnetic correlations. Susceptibility in mixed-valent TmSe shows similar antiferromagnetic ordering when both the 2+ and 3+ configurations are magnetic [30].

4. Conclusion

The effect of EPI has been studied using extended Falicov-Kimball model in an exact method. It appears that EPI enhances the tendency to an abrupt transition. The transition region is identified from the entropy curves. Temperature dependence of specific heat curves shows double peak structure. EPI increases the peak value of specific heat. Specific heat coefficient γ rises sharply at low temperatures. The peak value of γ decreases with EPI, preventing the onset of heavy-fermion behavior. Single peak structure in spin susceptibility curve signals the onset of short range antiferromagnetic order. EPI increases the rate of growth of antiferromagnetic correlations.

Acknowledgment

We are grateful to the University of Kalyani for financial help.

REFERENCES

1. **L.M.Falicov, J.C.Kimball,** Phys. Rev. Lett., **22,** 997 (1969).
2. **J.Freericks, V.Zlatic,** Rev. Mod. Phys., **75,** 1333 (2003).
3. **Ch.Gruber, M.Macris,** Helv. Phys. Acta B, **69,** 851 (1996).
4. **D.L.Khomskii,** Electronic phase transitions and the problem of mixed valence, in *Quantum Theory of Solids,* **M.Lifshitz, Ed.**, Mir, Moscow, 1982.
5. **G.Czycholl,** Phys. Rep., **143,** 277 (1986).
6. **J.M.Robinson,** Physics Rep., **51,** 1 (1979.)
7. **N.K.Ghosh, R.L.Sarkar,** Phys. Stat. Sol. (b), **176,** 395 (1993).
8. **H.Čenčarikova, P.Farkašovský,** Physica B, **359,** 690 (2005).
9. **N.K.Ghosh, S.K.Bhowmick, N.S.Mondal,** Pramana-J. Phys., **76,** 139 (2011).
10. **H.Čenčarikova, P.Farkašovský, M.Zonda,** Int. J. of Mod. Phys. B, **22**, 2473 (2008).
11. **O.L.T. de Menezes, and A.Troper,** Phys. Rev. B, **22**, 2127 (1980).
12. **P.Calvani, M.Capizzi, S.Lupi, P.Maselli, A.Paolone, P.Roy,** Phys. Rev. B, **53,** 2756 (1996).
13. **K.M.Shen, et. al.,** Phys. Rev. Lett., **93,** 267002 (2004).
14. **E.G.Maksimov, M.L.Kulic, O.V.Dolgov,** http://arxiv.org/abs/1001.4859.
15. **A.Lanzara, et. al.,** Nature, **412,** 510 (2001).
16. **A.P.G.Kutty,** J. Phys. Chem. Solids, **45**, 121 (1984).
17. **S.C.Ghosh, N.K.Ghosh, R.L.Sarkar,** Phys. Stat. Sol. (b), **161,** 661 (1990).

18. **P.Farkasovsky,** Z. Phys. B, **104,** 147 (1997).
19. **J.Bouvier, J.Bok,** Advances in Condensed Matter Physics, **2010**, article ID 472636 (2010).
20. **P.Entel, H.J.Leder, N.Grewe,** Z. Phys. B, **30**, 277 (1978).
21. **M. D.Nunez-Regueiro, M.Avignon,** J. Magn. Magn. Mater., **47**, 302 (1985).
22. **W.Hanke, J.E.Hirsch,** Phys. Rev. B, **25**, 6748 (1982).
23. **G.Czycholl,** Phys. Rep., **246,** 401 (1986).
24. **P.Farkasovsky,** Z. Phys. B, **104,** 553 (1997).
25. **N.S.Mondal, N.K.Ghosh,** Pramana-J. Phys., **74**, 1009 (2010).
26. **S.D.Bader, N.E.Phillips, D.B.McWhan,** Phys. Rev. B, **7**, 4686 (1973).
27. **C.Kittel,** Introduction to Solid State Physics, Wiley India Pvt. Ltd., New Delhi, 7th Edition, 2007, p. 156.
28. **G.R.Stewart,** Rev. Mod. Phys., **56**, 755 (1984).
29. **P.D.Sacramento,** J. Phys. Condens. Matter, **7**, 143 (1995).
30. **C.M.Varma,** Rev. Mod. Phys. **48**, 219 (1976).